

Fully amorphous atactic and isotactic block copolymers and their self-assembly into nano- and microscopic vesicles

Riccardo Wehr,¹ Elena C. dos Santos,¹ Moritz Muthwill,¹ Vittoria Chimisso,¹ Jens Gaitzsch,^{1,2,*} Wolfgang Meier^{1,*}

¹ University of Basel, Department of Chemistry, Mattenstrasse 24a, BPR 1096, 4058 Basel, Switzerland

² Leibniz-Institut für Polymerforschung Dresden e.V., Hohe Strasse 6, 01069 Dresden, Germany

* Corresponding Authors: gaitzsch@ipfdd.de, wolfgang.meier@unibas.ch

Supporting Information

Contents

1.1 Materials.....	2
1.2 Determination of the enantiomeric excess (<i>ee</i>) of the BO monomers.....	2
1.3 Syntheses.....	3
1.4 OmpF expression and purification	5
1.5 OmpF dialysis.....	6
2. Synthesis of atactic and isotactic homopolymers and BCPs	7
3. Characterisation of atactic and isotactic homopolymers and BCPs.....	10
3.1. ¹ H and ¹³ C NMR spectra.....	10
3.2. GPC elugrams	13
3.3. Content of meso and racemic diads.....	13
3.4. Polarimetry	14
3.4. CD-Spectroscopy	14
3.6. TGA and DSC thermograms.....	15
4. Self-assembly into SUVs	16
4.1. TEM images before extrusion.....	16
4.2. Dynamic and static light scattering before extrusion	16
4.3. Dynamic and static light scattering after extrusion	18
4.4. Cryo-TEM images after extrusion.....	19
4.5. TEM images 7 days after extrusion	20
4.6. Degree of stretching for the PBO and PDMS blocks ⁶	20
5. OmpF insertion and enzyme reaction	21

1. Experimental

1.1 Materials

The microwave vials used for the polymerisations were dried overnight at 120 °C prior to use. Potassium *tert*-butoxide (KO^tBu, ≥98%), 1,4,7,10,13,16-hexaoxacyclooctadecane (18-crown-6, ≥99%), racemic 1,2-butylene oxide (BO, 99%), ethyl vinyl ether (EVE, ≥98%), racemic glycidol (96%), calcium hydride (CaH₂, 95%), potassium (K, chunks in mineral oil, 98%) and naphthalene (Naph, 99%) were purchased from Sigma-Aldrich (Switzerland) and used as received. The enantiopure monomers (*R*- and (*S*)-1,2-butylene oxide (98%, ee unknown) as well as (*R*- and (*S*)-glycidol (97%, ee 98%) were purchased from Sigma-Aldrich (Switzerland), dried over CaH₂ and distilled prior to use. Dry solvents for the reactions were obtained from an inert solvent purification system PureSolv MD 5 (Inert Technology, USA) or from Acros Organics (Belgium). The other solvents were in HPLC grade and purchased from JT Baker (USA), VWR (Switzerland) or Scharlau (Germany). Deionised water was obtained from a MilliQ Q-POD device (Merck, Germany). Phosphate-buffered saline (PBS) was prepared in house using 8 g/L NaCl, 0.2 g/L KCl, 1.44 g/L Na₂HPO₄ and 0.24 g/L KH₂PO₄. Potassium naphthalenide (KNaph) was prepared by adding potassium (1.19 g, 30.5 mmol, 1eq) to a stirred solution of naphthalene (4.11 g, 32.0 mmol, 1.05 eq) in dry THF (61 mL, 0.5 mol/L) under nitrogen. Racemic and enantiopure EEGE was synthesized according to the standard protocol¹ from racemic or enantiopure glycidol and EVE, dried over CaH₂ and distilled prior to use. All reactants were stored under nitrogen atmosphere in a glovebox (MBraun Labstar, Germany).

1.2 Determination of the enantiomeric excess (*ee*) of the BO monomers

Figure S1 illustrates why the *ee* of the enantiopure BO monomers could not be determined using chiral gas chromatography (GC). To evaluate the ability of chiral GC to separate the (*S*)- from the (*R*)-BO monomer the racemic mixture of BO was analysed first. An elution already after 3.1 min was observed due to the high volatility of BO with its low boiling point of 63 °C. The segregation into two peaks for (*S*)- and (*R*)-BO was visible, but not baseline-separated and insufficient to determine the *ee*. When running (*S*)-BO, the obtained peak overlaid with the one of the (*S*)-BO from the racemic mixture. A peak corresponding to the (*R*)-enantiomer is not visible, indicating a high *ee*. Quantification was however not possible with the setup employed here. Other methods to measure the *ee* were not accessible. Since the quantification of the meso content of the polymers was successful, the exact *ee* of the monomer was not relevant in this case.

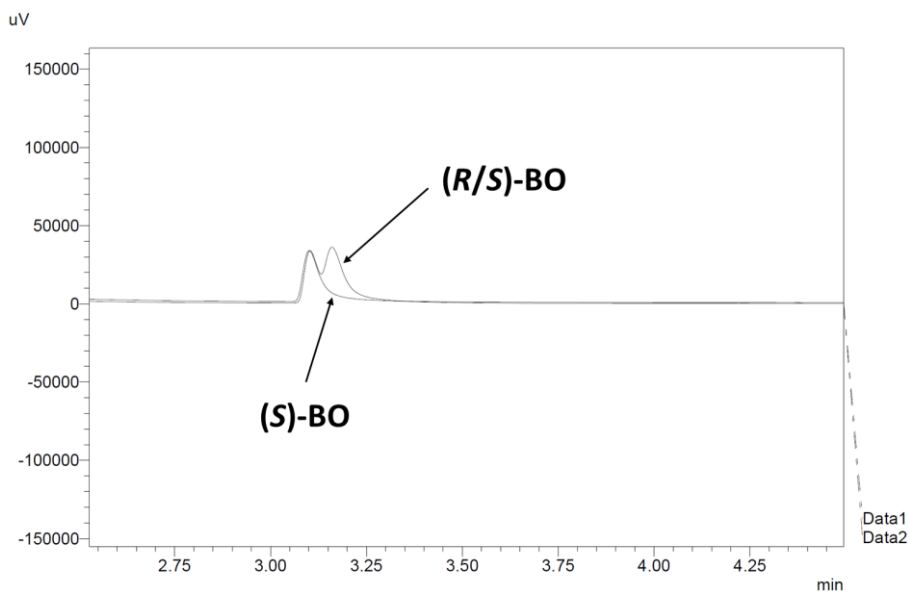


Figure S1: Chromatogram of (*R/S*)-BO and (*S*)-BO measured by chiral GC (2 mg/mL in pentane, Restek Rtx-5 column, 30 m, 0.25 mmID, 0.25 μ m df).

1.3 Syntheses

Synthesis of poly(butylene oxide) (PBO). The synthesis is described for the racemic (*R/S*)-PBO₂₇. The isotactic (*S*)-PBO₂₇ and (*R*)-PBO₂₇ were synthesised similarly, using the same protocol and scales, by replacing the racemic (*R/S*)-BO by the respective enantiopure analogues. Potassium *tert.* butoxide solution (KO^tBu, 0.25 mol/L in 1,4-dioxane, 9.25 mL, 2.31 mmol, 1 eq) was transferred into a 20 mL microwave vial equipped with a magnetic stirrer in a glovebox under nitrogen. Afterwards, a solution of 18-crown-6 (0.50 mol/L in 1,4-dioxane, 2.31 mL, 1.16 mmol, 0.5 eq) was added. The vial was closed and removed from the glovebox together with a syringe filled with racemic 1,2-butylene oxide ((*R/S*)-BO, 5.00g, 6.03 mL, 69.3 mmol, 30 eq). After adding (*R/S*)-BO to the reaction mixture through the septum of the lid, the microwave-assisted reaction was immediately started. A stepwise temperature increase was necessary in order to prevent the system from shutdown due to the slow heating rate caused by the high volume of the reaction solution. The following temperature program was applied: First heating step (two minutes at 50 °C), second heating step (two minutes at 60 °C), third heating step (30 min at 70 °C). After cooling to room temperature, methanol (2 mL) was added and stirred overnight to quench the reaction and to obtain hydroxy end groups. Subsequently, the solvents and unreacted monomer were evaporated using a rotary evaporator. The hydrophobic polymer, dissolved in *n*-hexane (100 mL), was washed with methanol (100 mL) in order to remove hydrophilic side products. The bottom, methanol enriched phase was then extracted three more times with *n*-hexane (each 100 mL). The combined *n*-hexane phases were then concentrated on a rotary evaporator. After drying overnight in high vacuum (0.05 mbar) the polymer was characterised and stored in a glovebox under nitrogen. 4.60 g (92%, M_n (NMR) = 2000 g/mol, 1.51 mmol, \bar{D} (GPC) = 1.08) of colourless, viscous (*R/S*)-PBO₂₇ were obtained.

(*R/S*)-PBO₂₇: ¹H-NMR (500 MHz, MeOD, 295 K, δ , ppm): 0.99 (m, 82H, -CH₂-CH₃), 1.23 (s, 9H, (H₃C)₃C-O-), 1.50–1.72 (m, 53H, -CH₂-CH₃), 3.39 (m, 27H, -CH₂-CH(CH₂-CH₃)-O-), 3.52 (m, 27H, -CHH_{cis}-CH(CH₂-CH₃)-O-), 3.67 (m, 26H, -CHH_{trans}-CH(CH₂-CH₃)-O-).

(*S*)-PBO₂₇: ¹H-NMR (500 MHz, MeOD, 295 K, δ , ppm): 0.99 (m, 84H, -CH₂-CH₃), 1.23 (s, 9H, (H₃C)₃C-O-), 1.50–1.72 (m, 55H, -CH₂-CH₃), 3.39 (m, 26H, -CH₂-CH(CH₂-CH₃)-O-), 3.54 (m, 26H, -CHH_{cis}-CH(CH₂-CH₃)-O-), 3.68 (m, 25H, -CHH_{trans}-CH(CH₂-CH₃)-O-).

(*R*)-PBO₂₇: ¹H-NMR (500 MHz, MeOD, 295 K, δ , ppm): 0.99 (m, 83H, -CH₂-CH₃), 1.23 (s, 9H, (H₃C)₃C-O-), 1.50–1.72 (m, 54H, -CH₂-CH₃), 3.39 (m, 26H, -CH₂-CH(CH₂-CH₃)-O-), 3.54 (m, 26H, -CHH_{cis}-CH(CH₂-CH₃)-O-), 3.67 (m, 25H, -CHH_{trans}-CH(CH₂-CH₃)-O-).

Synthesis of poly(butylene oxide)-block-poly(glycidol) (PBO-*b*-PG). The synthesis is described for the all-racemic (*R/S*)-PBO₂₆-*b*-(*R/S*)-PG₁₄. The isotactic (*S*)-PBO₂₇-*b*-(*S*)-PG₁₄ and (*R*)-PBO₂₆-*b*-(*R*)-PG₁₄ were synthesised similarly, using the same protocol and scales, by replacing the racemic (*R/S*)-EEGE by the respective enantiopure analogues. (*R/S*)-PBO₂₇ (0.65 g, 0.32 mmol, 1 eq) was transferred into a 5 mL microwave vial equipped with a magnetic stirrer in a glovebox under nitrogen. Then, 1,4-dioxane (2.61 mL) was added and the vial was closed and shaken. Potassium naphthalenide (KNaph, 0.5 mol/L in THF, 0.64 mL, 0.32 mmol, 1 eq) was added to the solution dropwise under shaking through the septum of the lid. The equivalence point of the titration was determined visually by a dark green color of the solution that remained for at least two minutes. After stirring for another five minutes, the reaction vial and a syringe filled with (*R/S*)-EEGE (0.64 g, 0.79 mL, 4.83 mmol, 15 eq) were removed from the glovebox. The monomer was added through the lid and the microwave-assisted polymerisation was immediately started. After running the reaction for 2.5 h at 70 °C, the vial was cooled to room temperature and the polymerisation was quenched overnight by adding methanol (0.5 mL). The solvents were evaporated using a rotary evaporator and the acetal protecting groups of the crude copolymer were cleaved in 0.1M HCl in ethanol (20 mL) for 3 h. The acidic solution was then neutralised using 1 M NaOH in ethanol. After partly removing the solvent on a rotary evaporator, the same volume MilliQ water was added. The copolymer solution was then transferred into a regenerated cellulose dialysis membrane with a MWCO of 1 kDa (RC6, Spectra Por, USA) and dialysed for two days against a 1:1 water:ethanol mixture. After five exchanges of the solvent mixture, two more dialysis steps against pure water were performed. Eventually, the copolymer dispersion was lyophilised overnight. 922 mg (95%, M_n (NMR) = 3000 g/mol, 0.31 mmol, \bar{D} (GPC) = 1.06) of colourless solid (*R/S*)-PBO₂₇-*b*-(*R/S*)-PG₁₄ were obtained.

(*R/S*)-PBO₂₆-*b*-(*R/S*)-PG₁₄: ¹H-NMR (500 MHz, MeOD, 295 K, δ , ppm): 0.97 (m, 79H, -CH₂-CH₃), 1.21 (s, 9H, (H₃C)₃C-O-), 1.45–1.69 (m, 52H, -CH₂-CH₃), 3.37 (m, 25H, -CH₂-CH(CH₂-CH₃)-O-), 3.46–3.85 (m, 123H, -CH₂-CH(CH₂-CH₃)-O-, -CH₂-CH(CH₂-OH)-O-).

(*S*)-PBO₂₇-*b*-(*S*)-PG₁₄: ¹H-NMR (500 MHz, MeOD, 295 K, δ , ppm): 0.97 (m, 83H, -CH₂-CH₃), 1.21 (s, 9H, (H₃C)₃C-O-), 1.45–1.69 (m, 55H, -CH₂-CH₃), 3.37 (m, 28H, -CH₂-CH(CH₂-CH₃)-O-), 3.46–3.85 (m, 125H, -CH₂-CH(CH₂-CH₃)-O-, -CH₂-CH(CH₂-OH)-O-).

(*R*)-PBO₂₆-*b*-(*R*)-PG₁₄: ¹H-NMR (500 MHz, MeOD, 295 K, δ , ppm): 0.97 (m, 79H, -CH₂-CH₃), 1.21 (s, 9H, (H₃C)₃C-O-), 1.45–1.69 (m, 52H, -CH₂-CH₃), 3.37 (m, 25H, -CH₂-CH(CH₂-CH₃)-O-), 3.46–3.85 (m, 123H, -CH₂-CH(CH₂-CH₃)-O-, -CH₂-CH(CH₂-OH)-O-).

Synthesis of poly(glycidol) (PG). The synthesis is described for the racemic (*R/S*)-PG₃₀. The isotactic (*S*)-PG₃₀ and (*R*)-PG₂₈ were synthesised similarly, using the same protocol and scales, by replacing the racemic (*R/S*)-EEGE by the respective enantiopure analogues. Potassium *tert.* butoxide solution (KO^tBu, 0.25 mol/L in 1,4-dioxane, 0.73 mL, 0.18 mmol, 1 eq) was transferred into a 5 mL microwave vial equipped with a magnetic stirrer in a glovebox under nitrogen. The vial was closed and removed from

the glovebox together with a syringe filled with (*R/S*)-EEGE (0.80 g, 0.90 mL, 5.48 mmol, 30 eq). The monomer was added through the lid and the microwave-assisted polymerisation was immediately started. After running the reaction for 2.5 h at 70 °C, the vial was cooled to room temperature and the polymerisation quenched overnight by adding methanol (0.5 mL). The solvents were evaporated using a rotary evaporator and the acetal protecting groups of the crude polymer were cleaved in 0.1M HCl in ethanol (10 mL) for 3 h. The acidic solution was then neutralised using 1 M NaOH in ethanol. The solution was then transferred into a regenerated cellulose dialysis membrane with a MWCO of 1 kDa (RC6, Spectra Por, USA) and dialysed for two days against ethanol with four exchanges of the solvent and eventually dried in vacuum. 350 mg (88%, $M_n(\text{NMR}) = 2300 \text{ g/mol}$, 0.15 mmol, $\mathcal{D}(\text{GPC}) = 1.07$) of colourless waxy (*R/S*)-PG₃₀ were obtained.

(*R/S*)-PG₃₀: ¹H-NMR (500 MHz, MeOD, 295 K, δ , ppm): 1.24 (s, 9H, (H_3C)₃C-O-), 3.52–3.93 (m, 150H, -CH₂-CH(CH₂-OH)-O-).

(*S*)-PG₃₀: ¹H-NMR (500 MHz, MeOD, 295 K, δ , ppm): 1.23 (s, 9H, (H_3C)₃C-O-), 3.52–3.93 (m, 148H, -CH₂-CH(CH₂-OH)-O-).

(*S*)-PG₂₈: ¹H-NMR (500 MHz, MeOD, 295 K, δ , ppm): 1.24 (s, 9H, (H_3C)₃C-O-), 3.52–3.93 (m, 141H, -CH₂-CH(CH₂-OH)-O-).

1.4 OmpF expression and purification

Wild-type OmpF was produced according to a modification of a previously published protocol:² overnight precultures of *E. coli* BL21 (DE3) omp8³ were grown in 6 mL lysogeny broth (LB) with 100 mg/L ampicillin at 37 °C and 150 rpm. 1 L of main culture (Terrific Broth (TB) with 100 mg/L ampicillin in 2.5 L Thomson Ultra Yield® flasks) was inoculated with 2x6 mL overnight culture and grown up to an OD₆₀₀ of 1–2 (37 °C, 300 rpm). Isopropyl β -D-1-thiogalactopyranoside (IPTG) was added to a final concentration of 0.5 mM to induce the expression. Expression cultures were further grown at 20 °C overnight (ca. 16 h). For prevention of excess foam formation during expression, a drop of Antifoam 204 (Sigma-Aldrich) was added. Cells were harvested by centrifugation (20 min, 4 °C, 27,500 rcf), then pellets were resuspended in lysis buffer kept on ice (10 mL lysis buffer per 1 g of pellet; 20 mM Tris-HCl, 2.5 mM MgCl₂, 1 mM CaCl₂) and subsequently homogenised by high-pressure homogenisation for 3 runs at max. 1100 bars (EmulsiFlex®-C3, Avestin, Inc.). A spatula tip of RNase A and DNase I (Roche Diagnostics GmbH), respectively, were added to the lysis suspension for a 30 min incubation at 37 °C. Sonication was conducted on ice for 10x (2 mins pulse 2 sec with 1 min breaks, amplitude 50). 1 mL 20% SDS per 10 mL of lysate was added for 1 h incubation at 60 °C. Membrane fragments were separated by centrifugation at 50,000 rcf at 20 °C. Pellets were washed with 2x3 mL 20 mM phosphate buffer, resuspended with a Dounce homogeniser in 0.125% octyl glucopyranoside (OG) in 20 mM phosphate buffer (3 mL per 1 g of pellet), incubated 1 h at 37 °C and centrifuged for 40 min at RT. The last step was repeated using 3% OG in 20 mM phosphate buffer (1.5 mL per 1 g of pellet). The supernatant was analysed for concentration and purity of OmpF. Concentration was determined by UV/Vis spectroscopy (Nanodrop 2000c Spectrophotometer, Thermo Scientific) and calculated by Lambert-Beer's law ($\epsilon_{\text{OmpF, monomer}} = 54200 \text{ M}^{-1} \text{ cm}^{-1}$ or $\epsilon_{\text{OmpF, trimer}} = 162630 \text{ M}^{-1} \text{ cm}^{-1}$, $M_{\text{OmpF, monomer}} = 37.085 \text{ kDa}$).⁴ Purity was determined by the 260/280 absorbance ratio (≤ 0.6 , for absence of nucleic acid contamination) and by SDS-PAGE (12% gel), see Figure S2.

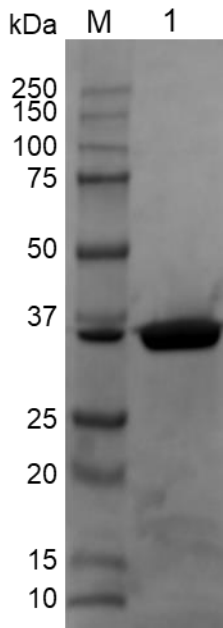


Figure S2: SDS-PAGE of purified OmpF. M: Marker (Precision Plus Protein standard), Lane 1: Purified OmpF in 3% OG. 10 μ g protein were boiled at 95 °C for 5 min in loading buffer (f.c. 2% SDS, 50 mM Tris-HCl pH 6.8, 10% glycerol, 0.004% bromophenol blue, 100 mM DTT).

1.5 OmpF dialysis

Before reconstituting OmpF, dialysis was conducted as previously published,⁵ using Spectrum™ Spectra/Por™ Float-A-Lyzer™ G2 dialysis tubes (1 ml, 20 kDa MWCO). Alternatively, after the first dialysis step against 0.05% OG overnight, the first dialysis step against pure PBS was conducted overnight, whereas the second dialysis step against PBS was conducted for 2 h, according to the standard protocol. If necessary, the dialysed OmpF in PBS was concentrated using the Spectra/Gel™ Absorbent. The final OmpF solution was either used freshly after dialysis, or stored at 4 °C maximum overnight for usage at the next day.

2. Synthesis of atactic and isotactic homopolymers and BCPs

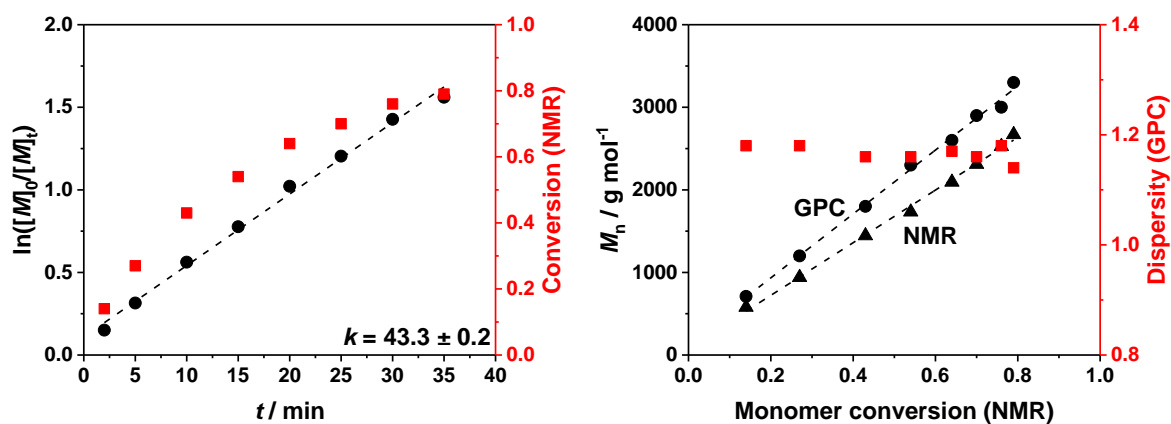


Figure S3: Kinetics of the (R/S)-PBO synthesis.

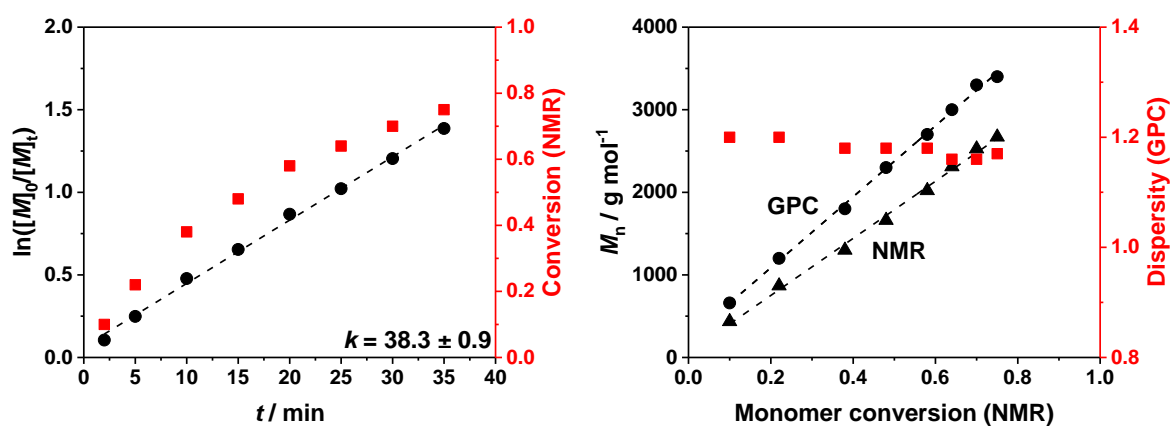


Figure S4: Kinetics of the (R)-PBO synthesis.

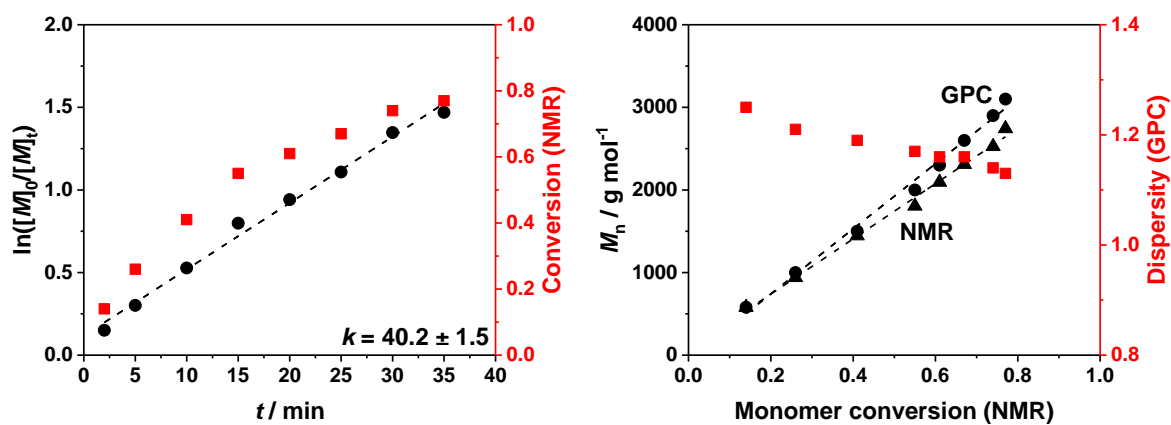


Figure S5: Kinetics of the (S)-PBO synthesis.

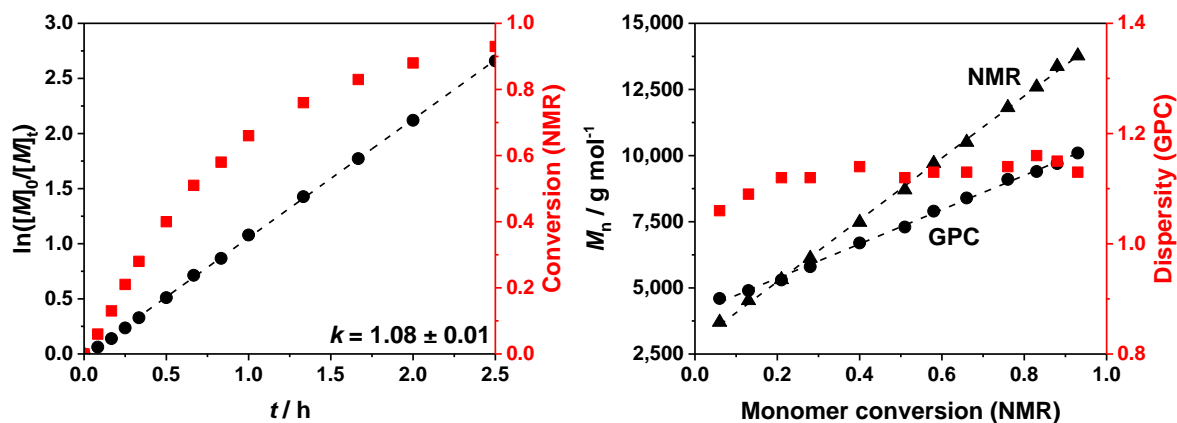


Figure S6: Kinetics of the (R/S)-PBO-*b*-(R/S)-PEEGE synthesis.

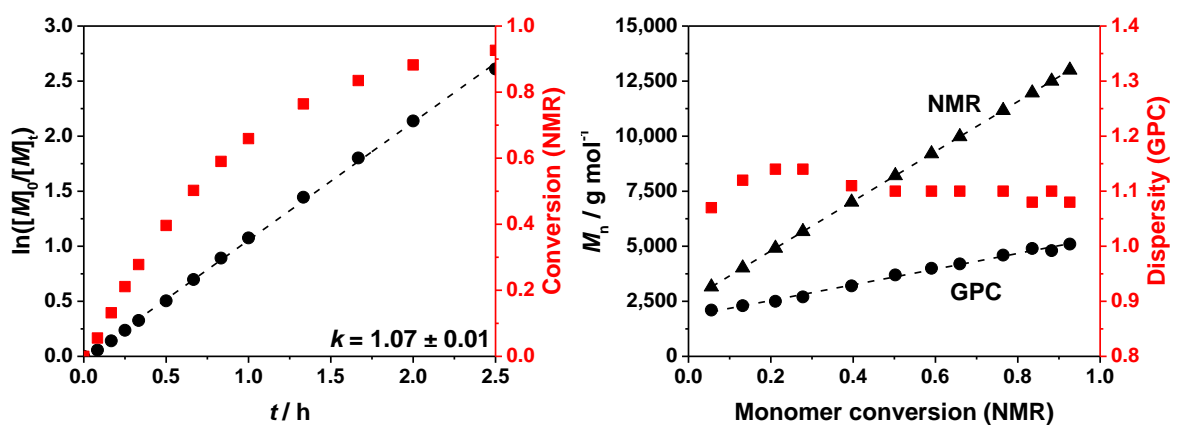


Figure S7: Kinetics of the (R)-PBO-*b*-(R)-PEEGE synthesis.

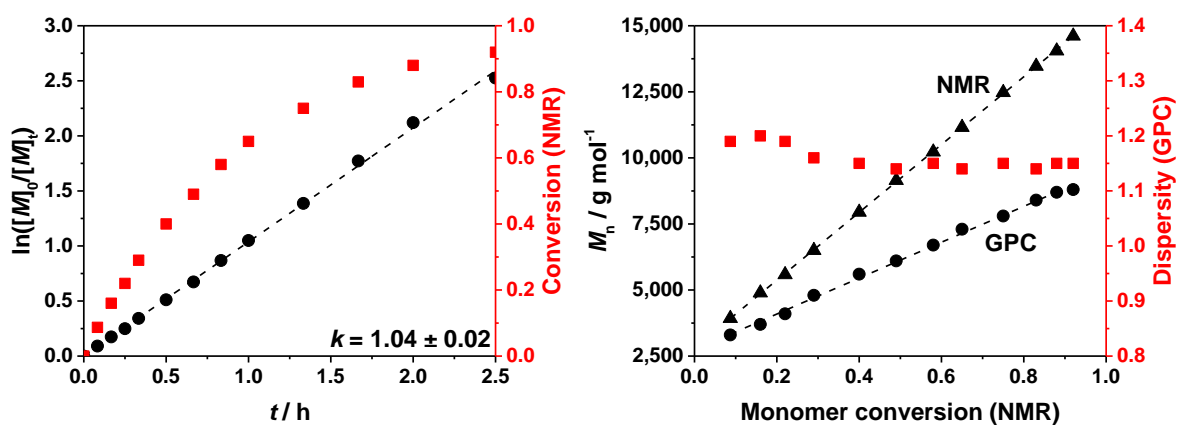


Figure S8: Kinetics of the (S)-PBO-*b*-(S)-PEEGE synthesis.

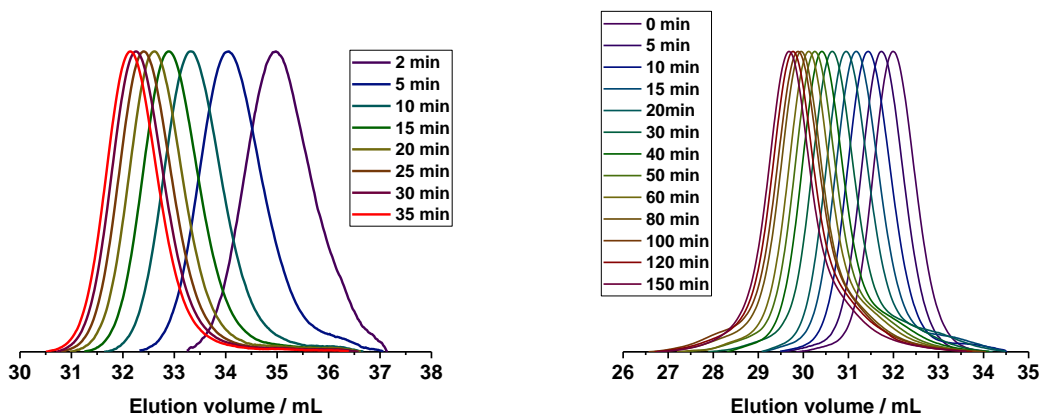


Figure S9: GPC traces of the kinetic measurements of (R/S)-PBO (left) and (R/S)-PBO-*b*-(R/S)-PEEGE (right).

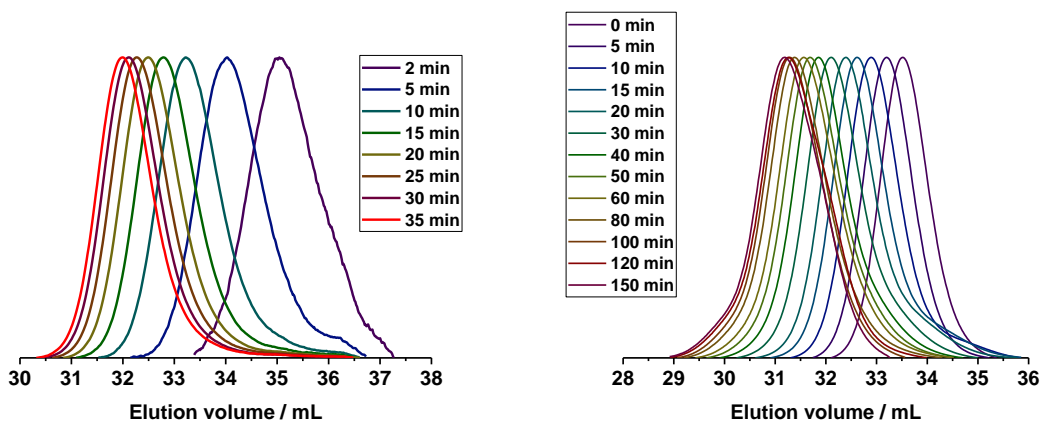


Figure S10: GPC traces of the kinetic measurements of (R)-PBO (left) and (R)-PBO-*b*-(R)-PEEGE (right).

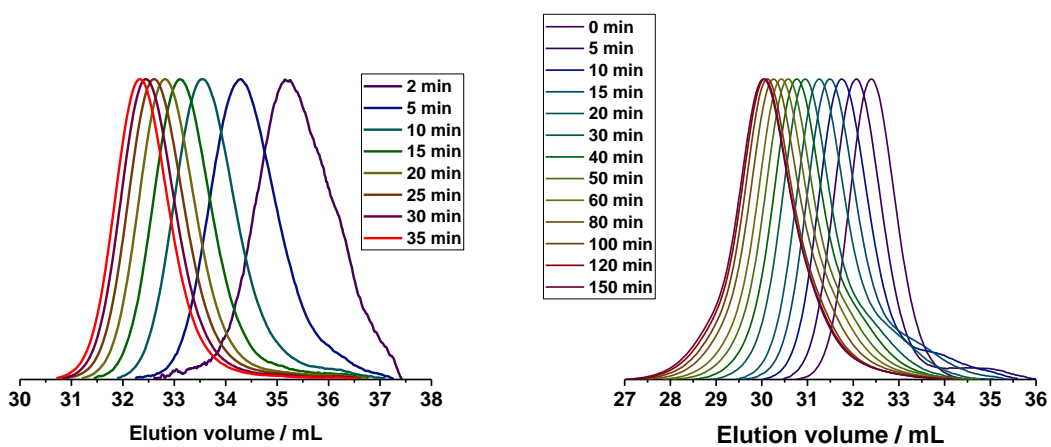


Figure S11: GPC traces of the kinetic measurements of (S)-PBO (left) and (S)-PBO-*b*-(S)-PEEGE (right).

3. Characterisation of atactic and isotactic homopolymers and BCPs

3.1. ^1H and ^{13}C NMR spectra

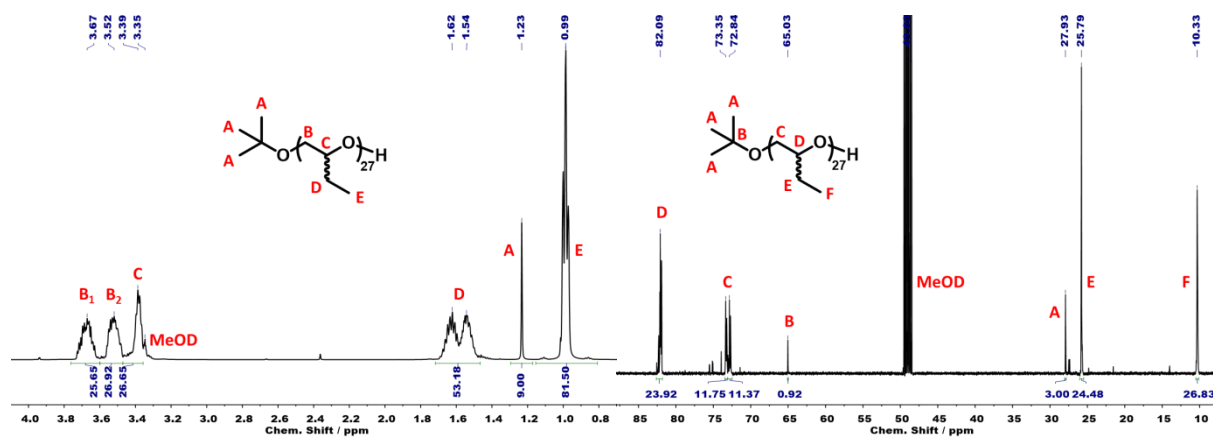


Figure S12: ^1H NMR spectrum (left) and ^{13}C NMR spectrum (right) of $(R/S)\text{-PBO}_{27}$ in MeOD.

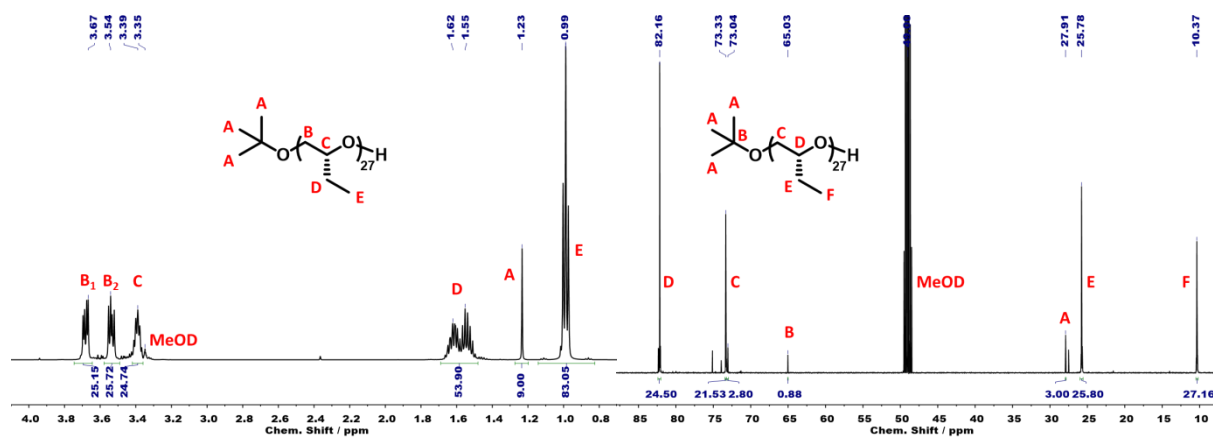


Figure S13: ^1H NMR spectrum (left) and ^{13}C NMR spectrum (right) of $(R)\text{-PBO}_{27}$ in MeOD.

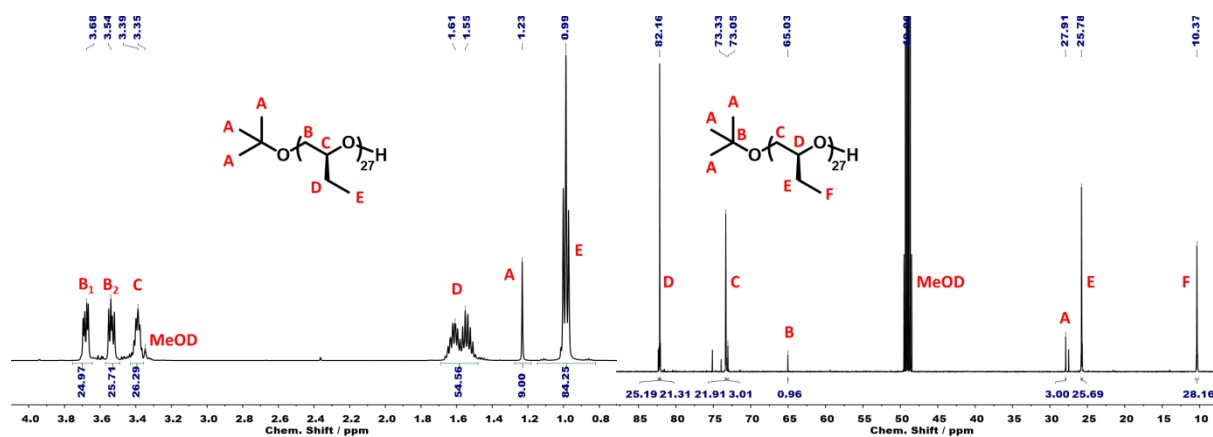


Figure S14: ^1H NMR spectrum (left) and ^{13}C NMR spectrum (right) of $(S)\text{-PBO}_{27}$ in MeOD.

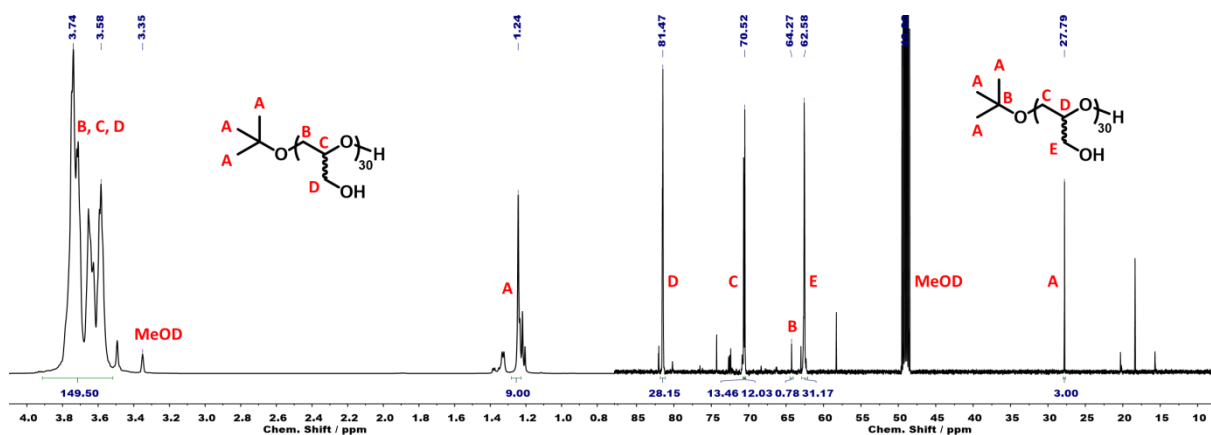


Figure S15: ^1H NMR spectrum (left) and ^{13}C NMR spectrum (right) of $(R/S)\text{-PG}_{30}$ in MeOD.

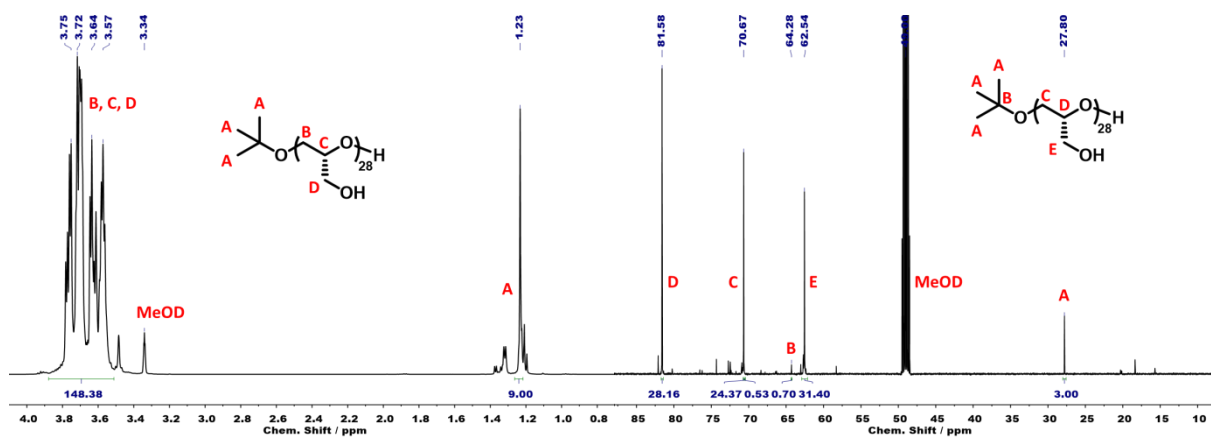


Figure S16: ^1H NMR spectrum (left) and ^{13}C NMR spectrum (right) of $(R)\text{-PG}_{28}$ in MeOD.

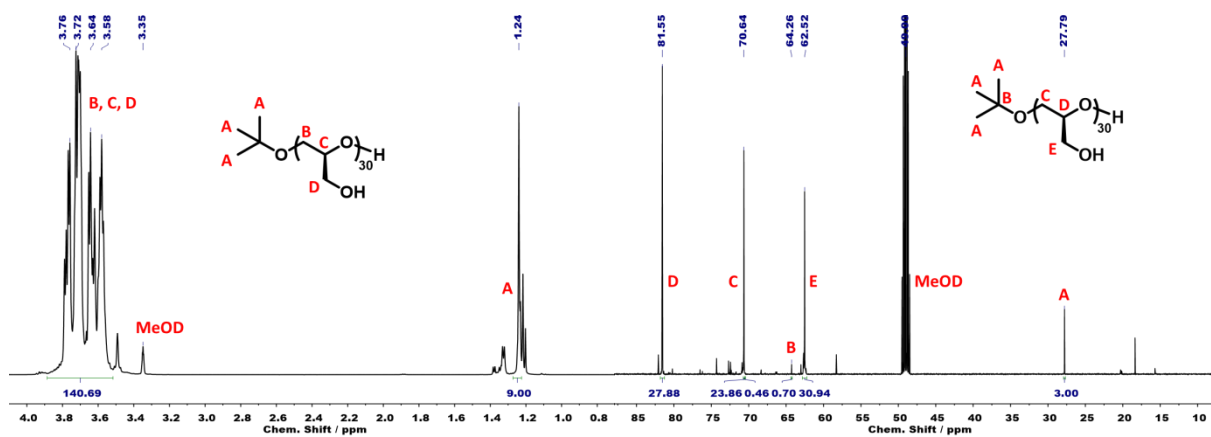


Figure S17: ^1H NMR spectrum (left) and ^{13}C NMR spectrum (right) of $(S)\text{-PG}_{30}$ in MeOD.

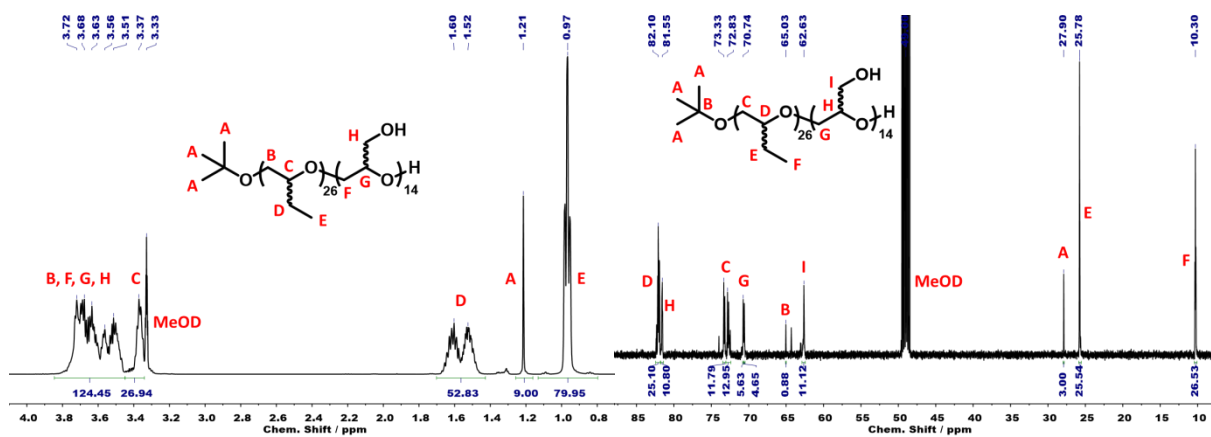


Figure S18: ^1H NMR spectrum (left) and ^{13}C NMR spectrum (right) of $(R/S)\text{-PBO}_{26}\text{-}b\text{-}(R/S)\text{-PG}_{14}$ in MeOD.

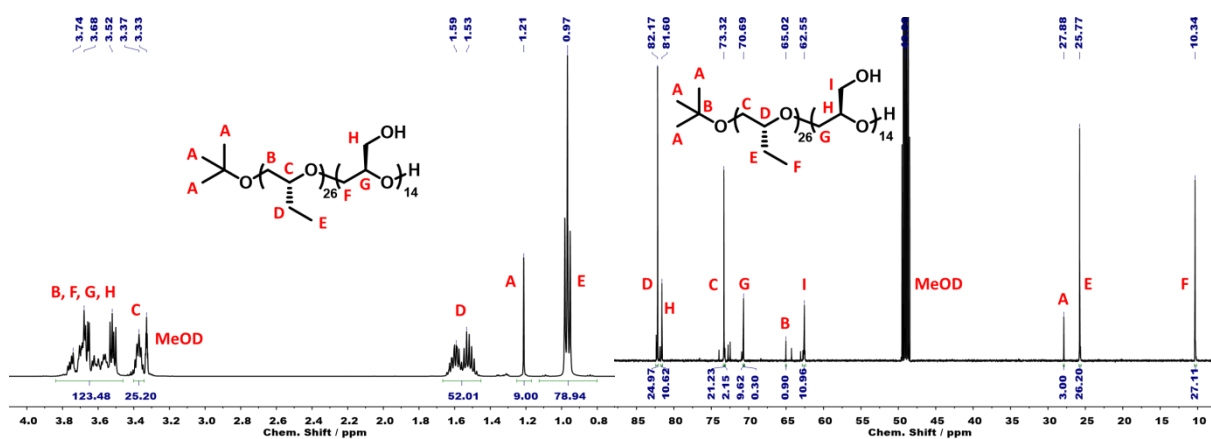


Figure S19: ^1H NMR spectrum (left) and ^{13}C NMR spectrum (right) of $(R)\text{-PBO}_{26}\text{-}b\text{-}(R)\text{-PG}_{14}$ in MeOD.

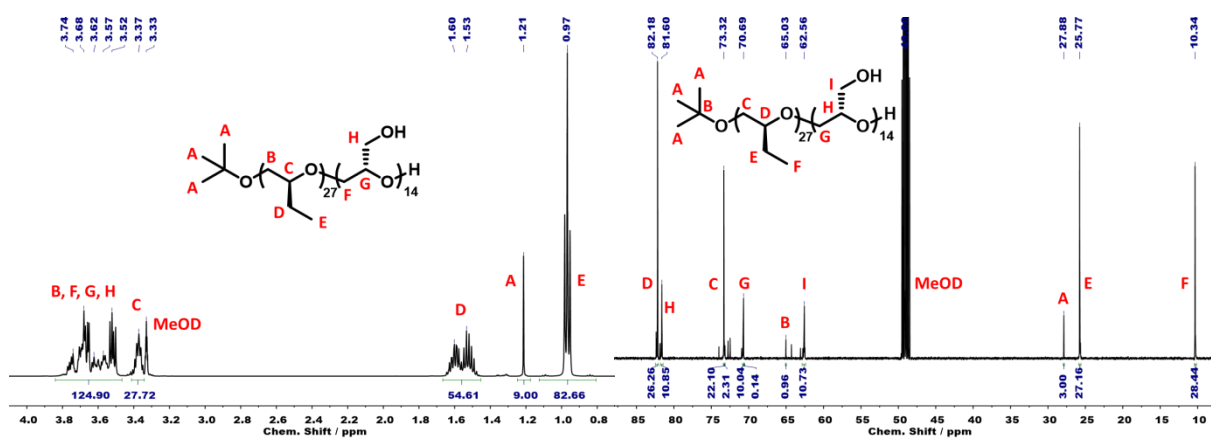


Figure S20: ^1H NMR spectrum (left) and ^{13}C NMR spectrum (right) of $(S)\text{-PBO}_{27}\text{-}b\text{-}(S)\text{-PG}_{14}$ in MeOD.

3.2. GPC elugrams

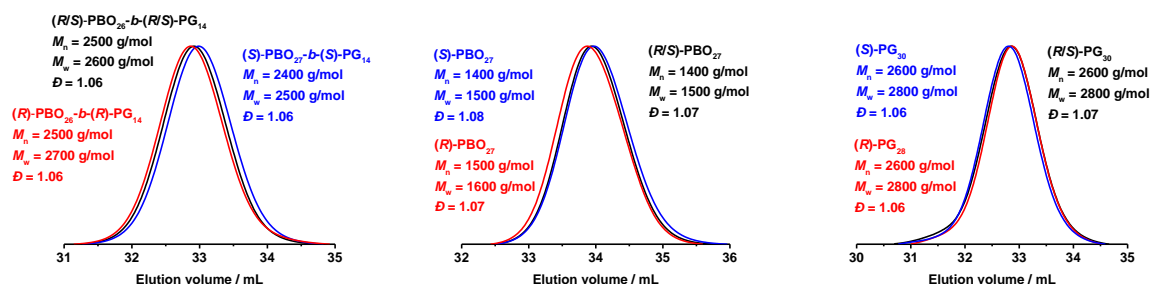


Figure S21: GPC traces of the atactic and isotactic PBO-*b*-PG copolymers (left), PBO homopolymers (middle) and PG homopolymers (right).

3.3. Content of meso and racemic diads

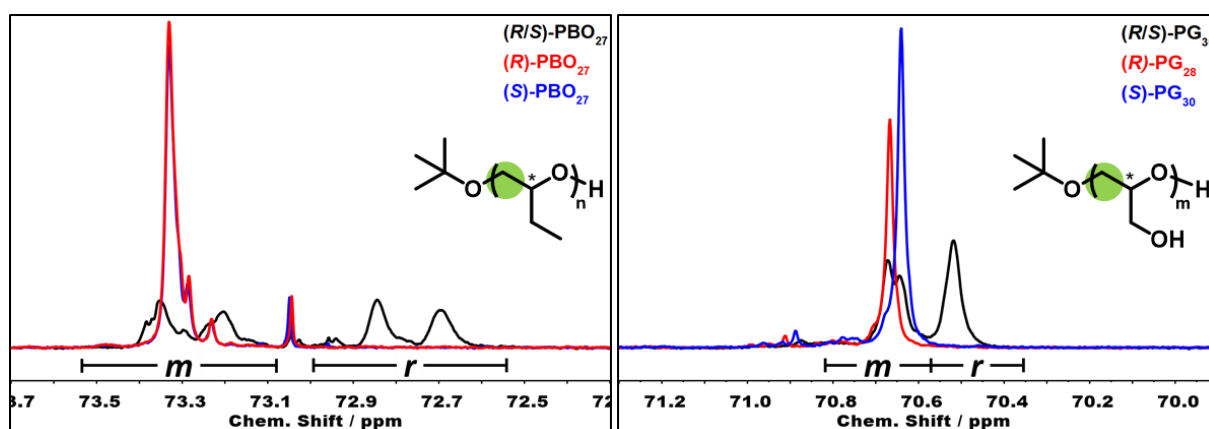


Figure S22: ^{13}C NMR signals of the methylene carbon atoms next to the chiral methine carbon atoms in the polymer backbone of the PBO homopolymer (left) and the PG homopolymer (right) indicated with a green circle. The integrated areas correspond to racemic (*r*) and meso (*m*) diads.

Table S1: Calculation of the content of meso diads (*m*) from the integrals of the ^{13}C NMR peaks at 71 ppm (PG blocks) and 73 ppm (PBO blocks), taken from Figures S12-S20.

polymer	$\int m$ (PBO)	$\int r$ (PBO)	$\int m$ (PG)	$\int r$ (PG)	<i>m</i> (PBO)	<i>m</i> (PG)
(<i>R/S</i>)-PBO ₂₆ - <i>b</i> -(<i>R/S</i>)-PG ₁₄	11.79	12.95	5.63	4.65	48%	55%
(<i>R</i>)-PBO ₂₆ - <i>b</i> -(<i>R</i>)-PG ₁₄	21.23	2.15	9.62	0.30	91%	97%
(<i>S</i>)-PBO ₂₇ - <i>b</i> -(<i>S</i>)-PG ₁₄	22.10	2.31	10.04	0.14	91%	99%
(<i>R/S</i>)-PBO ₂₇	11.75	11.37	–	–	51%	–
(<i>R</i>)-PBO ₂₇	21.53	2.80	–	–	88%	–
(<i>S</i>)-PBO ₂₇	21.91	3.01	–	–	88%	–
(<i>R/S</i>)-PG ₃₀	–	–	13.46	12.03	–	53%
(<i>R</i>)-PG ₂₈	–	–	24.37	0.53	–	98%
(<i>S</i>)-PG ₃₀	–	–	23.86	0.46	–	98%

3.4. Polarimetry

Table S2: Specific rotations of the racemic and enantiopure monomers measured by polarimetry.

compound	$[\alpha]_{25}^D$
(<i>R/S</i>)-BO	+0.0
(<i>R</i>)-BO	+7.2
(<i>S</i>)-BO	-6.4
(<i>R/S</i>)-glycidol	+0.3
(<i>R</i>)-glycidol	+11.6
(<i>S</i>)-glycidol	-12.0
(<i>R/S</i>)-EEGE	+0.0
(<i>R</i>)-EEGE	+9.9
(<i>S</i>)-EEGE	-9.6
(<i>R/S</i>)-PEEGE	-0.01
(<i>R</i>)-PEEGE	+10.0
(<i>S</i>)-PEEGE	-10.1

3.4. CD-Spectroscopy

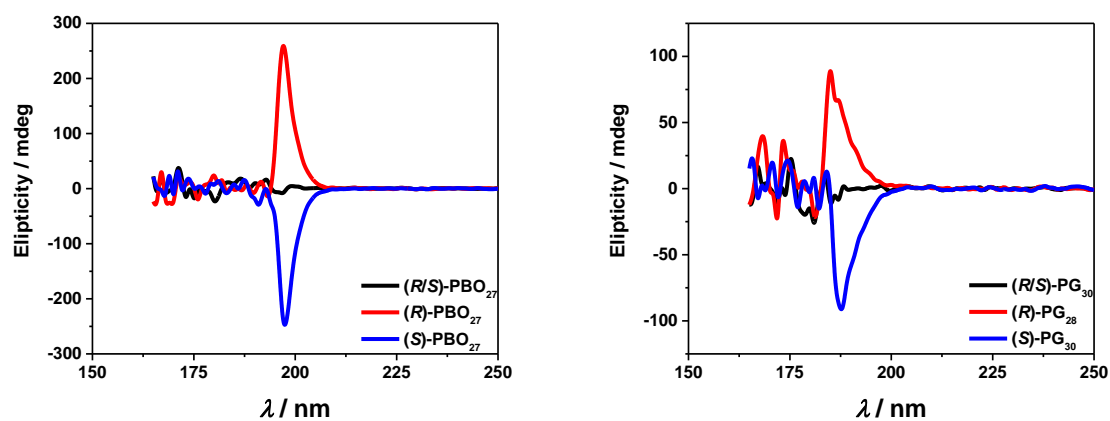


Figure S23: CD spectra of atactic and isotactic PBO (left) and PG (right) homopolymers.

3.6. TGA and DSC thermograms

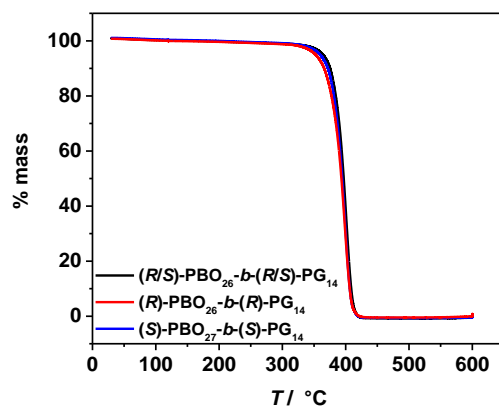


Figure S24: TGA thermogram of atactic and isotactic PBO-*b*-PGs. The mass loss was >99% for every polymer.

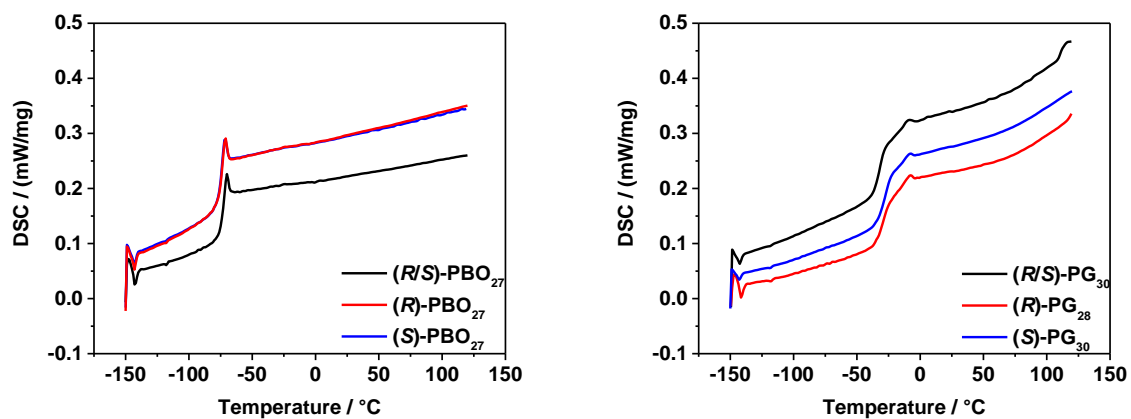


Figure S25: DSC thermograms of atactic and isotactic PBO homopolymers (left) and PG homopolymers (right).

4. Self-assembly into SUVs

4.1. TEM images before extrusion

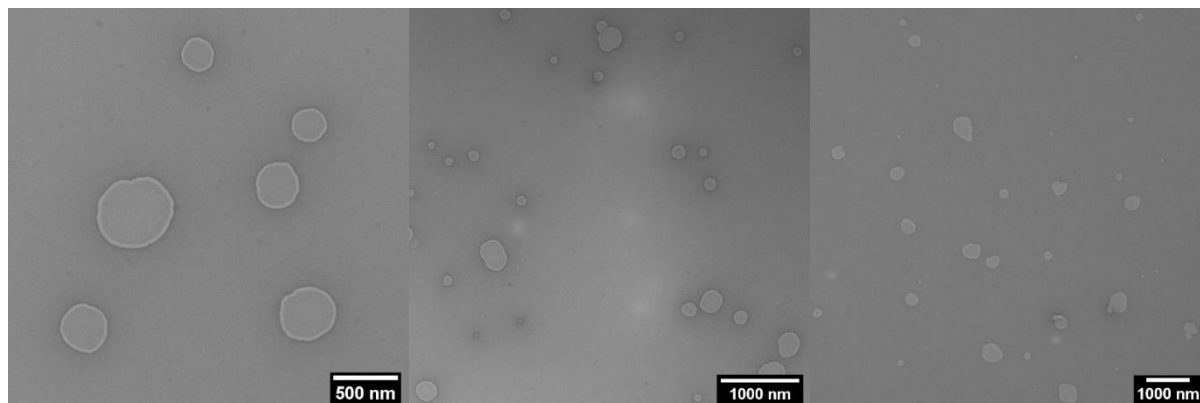


Figure S26: TEM images of (R/S) -PBO₂₆- b -(R/S)-PG₁₄ SUVs (left), (R) -PBO₂₆- b -(R)-PG₁₄ SUVs (middle) and (S) -PBO₂₇- b -(S)-PG₁₄ SUVs (right) before extrusion.

4.2. Dynamic and static light scattering before extrusion

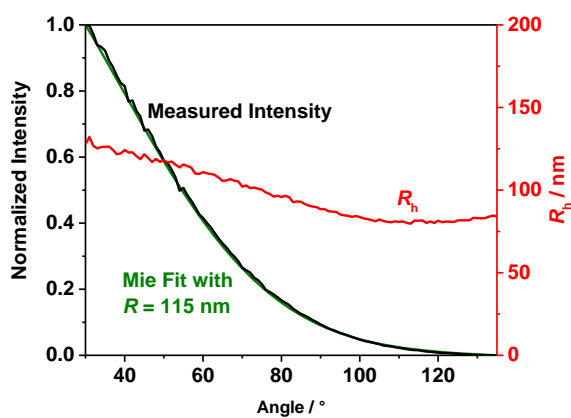


Figure S27: DLS and SLS data (Mie fit) of (R/S) -PBO₂₆- b -(R/S)-PG₁₄ SUVs before extrusion.

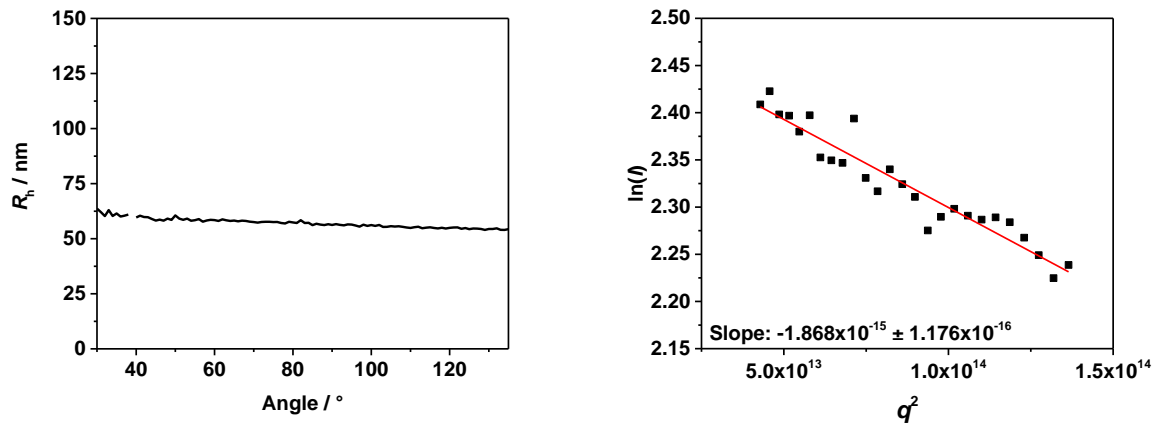


Figure S28: DLS and SLS data (guinier fit) of (R)-PBO₂₆-b-(R)-PG₁₄ SUVs before extrusion.

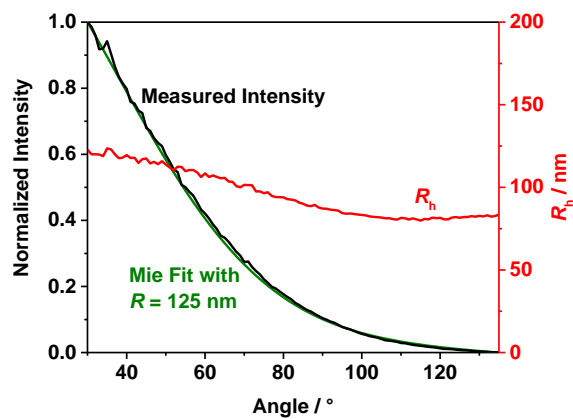


Figure S29: DLS and SLS data (Mie fit) of (S)-PBO₂₇-b-(S)-PG₁₄ SUVs before extrusion.

4.3. Dynamic and static light scattering after extrusion

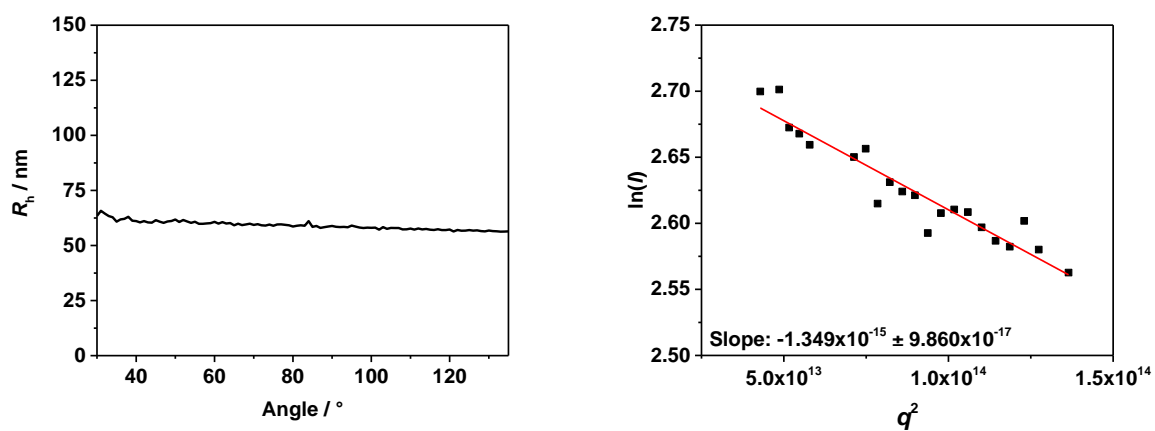


Figure S30: DLS and SLS data (Guinier fit) of (R/S)-PBO₂₆-b-(R/S)-PG₁₄ SUVs after extrusion with a 100 nm membrane.

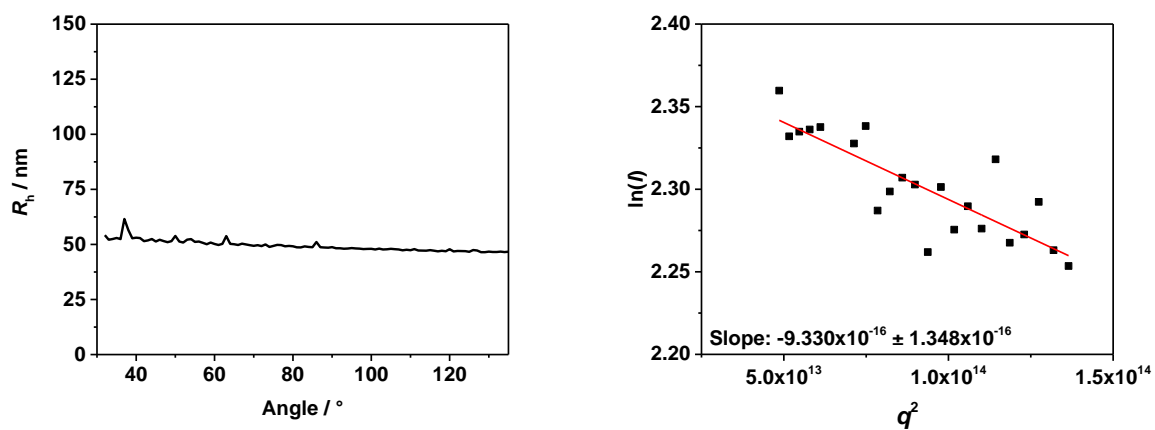


Figure S31: DLS and SLS data (Guinier fit) of (R)-PBO₂₆-b-(R)-PG₁₄ SUVs after extrusion with a 100 nm membrane.

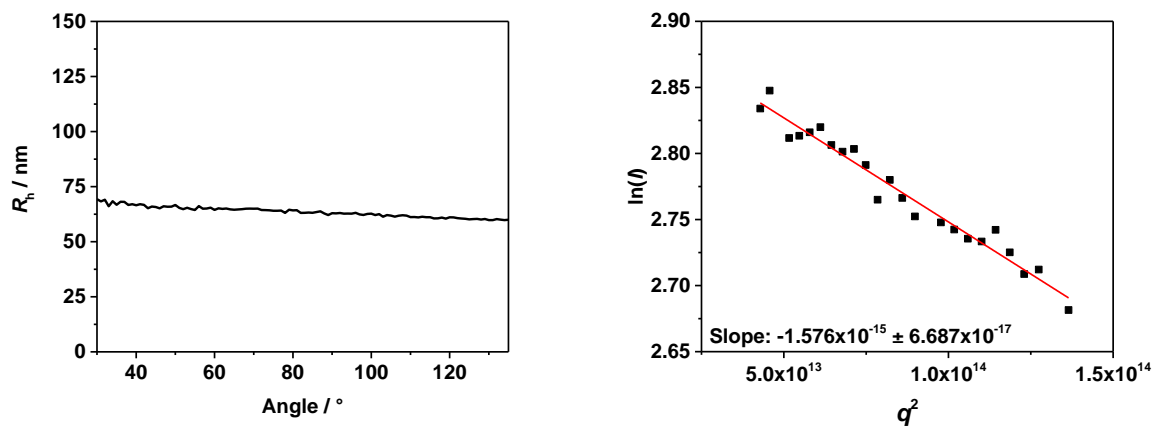


Figure S32: DLS and SLS data (Guinier fit) of (S)-PBO₂₇-*b*-(S)-PG₁₄ SUVs after extrusion with a 100 nm membrane.

4.4. Cryo-TEM images after extrusion

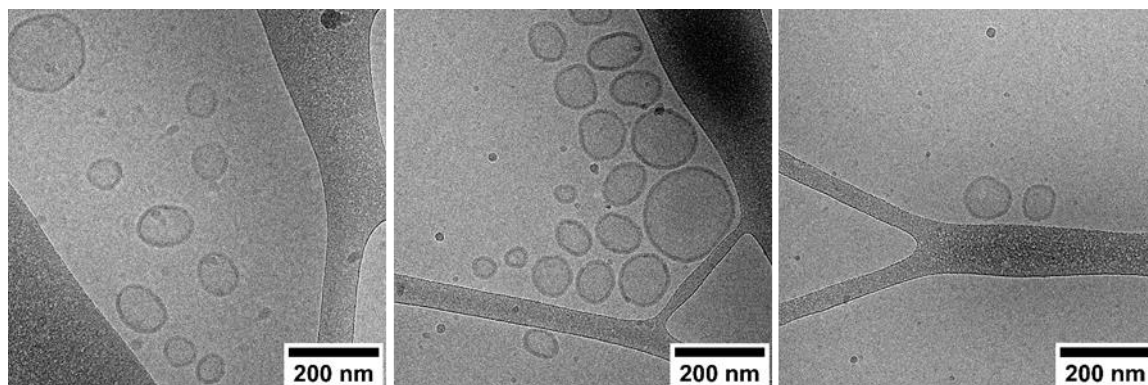


Figure S33: Cryo-TEM images of (R/S)-PBO₂₆-*b*-(R/S)-PG₁₄ SUVs (left), (R)-PBO₂₆-*b*-(R)-PG₁₄ SUVs (middle) and (S)-PBO₂₇-*b*-(S)-PG₁₄ SUVs (right), showing SUVs and micelles.

4.5. TEM images 7 days after extrusion

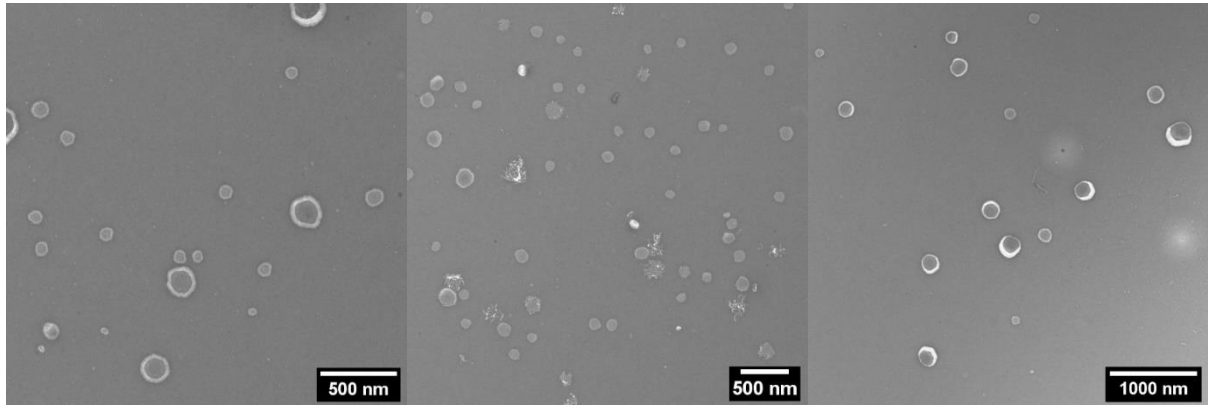


Figure S34: TEM images of (R/S)-PBO₂₆-b-(R/S)-PG₁₄ SUVs (left), (R)-PBO₂₆-b-(R)-PG₁₄ SUVs (middle) and (S)-PBO₂₇-b-(S)-PG₁₄ SUVs (right) after 7 days at room temperature.

4.6. Degree of stretching for the PBO and PDMS blocks⁶

For a fully stretched conformation the contour length $R_{contour}$ would be:

$$R_{contour} = l * n * d * \sin\left(\frac{\theta}{2}\right)$$

PBO₂₆ has 3 bonds per repeating unit (l) and 26 repeating units (n). Taking the bond length of PEO as a reference (d), this becomes for a tetrahedral bond angle (θ):

$$R_{contour} = 3 * 26 * 0.145 \text{ nm} * \sin\left(\frac{109.5}{2}\right) = 9.2 \text{ nm}$$

The end-to-end distance of a random coil-like conformation (R_{coil}) is given as

$$R_{coil} = \sqrt{\frac{1 - \cos\theta}{1 + \cos\theta}} * l * n * d$$

Taking the same values as above results for PBO₂₆ in

$$R_{coil} = \sqrt{\frac{1.33}{0.67}} * 3 * 26 * 0.145 \text{ nm} = 1.8 \text{ nm}$$

Effective conformation:

The side chain of PBO prevents an arrangement in a perfect coil-like conformation. However, a fully stretched conformation can also not be achieved. Consequently, it exhibits a mixed conformation of both components. The degree of stretching x can thus be calculated using the membrane thickness l (effective length $R_{eff} = l/2$ as it is a bilayer system) and the theoretical lengths $R_{contour}$ and R_{coil} as follows:

$$R_{eff} = x * R_{contour} + (1 - x) * R_{coil}$$

For PBO₂₆ x is accordingly

$$x = \frac{R_{eff} - R_{coil}}{R_{contour} - R_{coil}} = \frac{5.6 \text{ nm} - 1.8 \text{ nm}}{9.2 \text{ nm} - 1.8 \text{ nm}} = 51\%$$

--> PBO is 51% stretched in a bilayer membrane

5. OmpF insertion and enzyme reaction

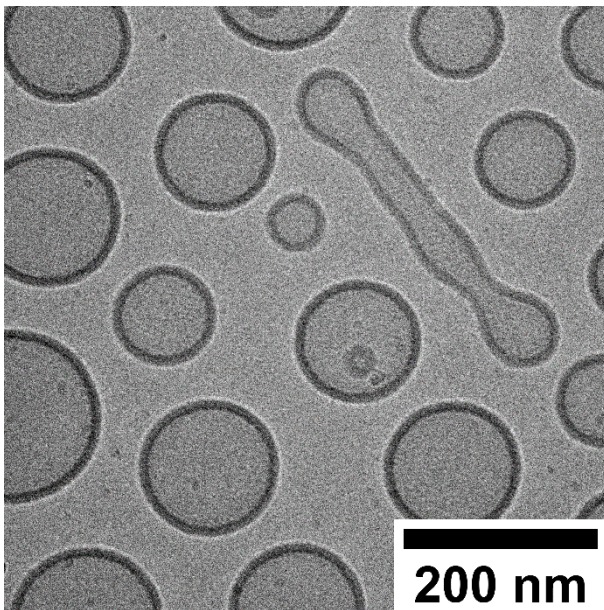


Figure S35: Exemplary Cryo-TEM image of PDMS₂₅-*b*-PMOXA₁₀ SUVs, prepared by film rehydration as published elsewhere⁷ and extruded with a 100 nm membrane. The Cryo-TEM images were used to determine the membrane thickness.

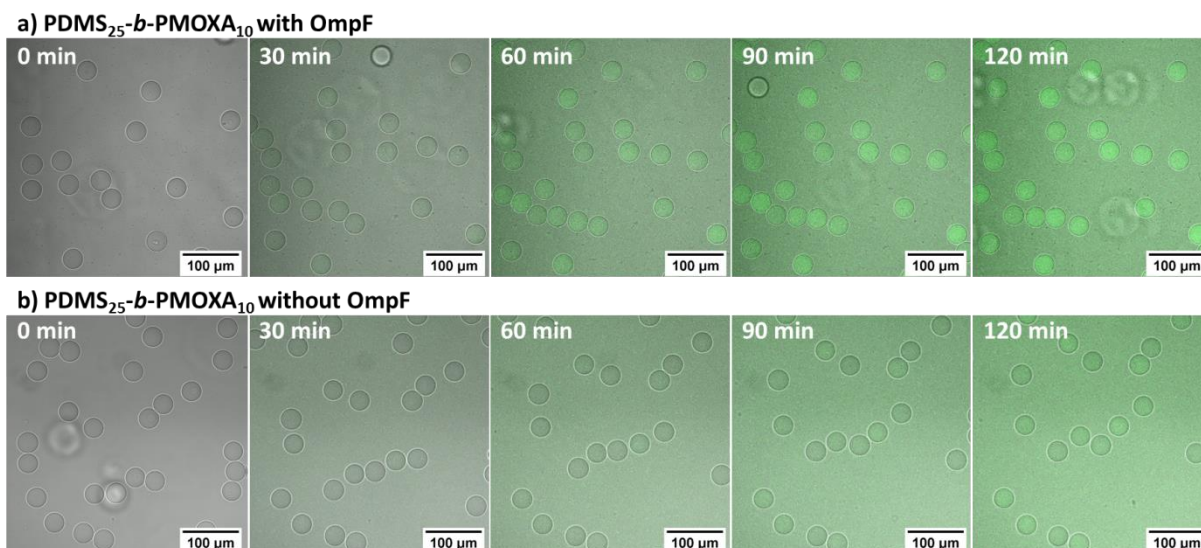


Figure S36: Kinetics of the enzyme reaction within the cavity of PDMS₂₅-*b*-PMOXA₁₀ GUVs a) with and b) without reconstituted membrane protein OmpF.

References

- 1 A. O. Fitton, J. Hill, D. E. Jane and R. Millar, *Synthesis (Stuttg.)*, 1987, **1987**, 1140–1142.
- 2 M. Grzelakowski, O. Onaca, P. Rigler, M. Kumar and W. Meier, *Small*, 2009, **5**, 2545–2548.
- 3 A. Prilipov, P. S. Phale, P. Van Gelder, J. P. Rosenbusch and R. Koebnik, *FEMS Microbiol. Lett.*, 1998, **163**, 65–72.
- 4 R. Chen, C. Krämer, W. Schmidmayr, U. Chen-Schmeisser and U. Henning, *Biochem. J.*, 1982, **203**, 33–43.
- 5 M. Garni, T. Einfalt, R. Goers, C. G. Palivan and W. Meier, *ACS Synth. Biol.*, 2018, **7**, 2116–2125.
- 6 D. Daubian, A. Fillion, J. Gaitzsch and W. Meier, *Macromolecules*, 2020, **53**, 11040–11050.
- 7 C. E. Meyer, I. Craciun, C. A. Schoenenberger, R. Wehr and C. G. Palivan, *Nanoscale*, 2021, **13**, 66–70.